Interaction Between Patch Loading, Bending, and Shear in Steel Girder Bridges Erected with the Incremental Launching Method

T. Andres Sanchez[1], Andres F. Robalino[2], Carlos Graciano[3]

Abstract

In the incremental launching method (ILM), a bridge structure is assembled behind one of the end supports and moved longitudinally, passing by intermediate piers until it reaches the other end support. As the structure moves forward, the cantilever length increases until the launching nose reaches the next pier or abutment. In this process, at the cantilever support, the steel girders are subject to a combination of stresses due to the reaction force (or patch loading), major-axis bending, and shear. This loading condition, known as the M-V-P interaction, may lead to high stress concentrations that may cause local instability in the steel girder panels located at the cantilever support, principally due to the high web slenderness ratios. This paper presents the strain/stress measurements obtained from a steel I-girder bridge erected with the ILM. The instrumentation was positioned at three different locations along one of the I-girders to capture the stress variation, as the bridge was launched. These measurements serve as the basis to better understand the M-V-P interaction in steel girder bridges erected with this method. In addition, the field measurements are compared to available analytical models that predict this interaction in steel I-girder bridges erected with the ILM.

Notation

B_{units} = vibrating wire strain gauge natural frequency

E = modulus of elasticity of steel

f_{bu} = flange major-axis bending stress

f_{ℓ} = flange lateral bending stress

F_c = vibrating wire strain gauge calibration factor

F_{crw} = nominal web bend-buckling resistance for webs

F_{nc} = nominal flexural resistance of the compression flange

F_{yc} = compression flange yield strength

F_{yt} = tension flange yield strength

---

[1] President, ADSTREN Cia. Ltda., <tasanchez@adstren.com>
[2] Structural Engineer, ADSTREN Cia. Ltda., <arobalino@adstren.com>
[3] Associate Professor, Universidad Nacional de Colombia, <cagraciano@unal.edu.co>

$M =$ bending moment acting on the girder

$M_n =$ nominal bending resistance

$M_R =$ bending resistance of the girder

$M_u =$ moment reaction at the section under consideration due factored loads

$P =$ applied patch load

$P_n =$ patch loading nominal resistance

$P_R =$ patch loading resistance of the loaded web panel

$P_u =$ vertical reaction at the section under consideration due factored loads

$R_h =$ hybrid factor

$R_{nc} =$ nominal web crippling strength

$R_{ny} =$ nominal web yielding strength

$R_u =$ factored concentrated load or bearing reaction

$Strain_{\mu\varepsilon} =$ vibrating wire micro-strain

$V =$ shear force acting on the loaded panel

$V_{cr} =$ shear-buckling resistance

$V_n =$ nominal shear resistance

$V_R =$ Shear buckling resistance of the loaded web panel

$V_u =$ shear in the web at the section under consideration due to factored loads

$\phi_b =$ resistance factor for bearing

$\phi_f =$ resistance factor for flexure

$\phi_v =$ resistance factor for shear

1. Introduction

The incremental launching method (ILM) is a procedure where the bridge structure is assembled behind one of the end supports, and then it is moved longitudinally to reach the next support. Normally, this technique is used to construct bridges with multiple spans even though there are cases where simple span structures have been erected with this method. During the launching process, the girders cantilever out from the support, which results in large deflections at the girders' free ends. To compensate for these large magnitude deflections, a launching nose is connected to free ends of at least two girders. The tapered shape of the nose's bottom flange is designed to compensate for the girder deflections, so the nose is able to land at the roller (or sliding surface) located at the next support.

In addition to substantial girder deflections, a bridge erected with the ILM may be subject to considerable strength demands. Large stress concentrations occur near the cantilever support due to the bending and shear demands in combination with a large vertical reaction. As the launching process advances, the major-axis bending moment, the vertical shear force, and the support point load increases, subjecting the steel girders to high stress levels that may compromise the structure's integrity, as shown in Figure 1.

Figure 1: Collapse of a bridge structure erected with the ILM

Current LRFD Bridge Design Specifications (AASHTO 2014) contains provisions to conduct the construction strength checks for flexure and shear separately. There is substantial experimental and analytical research that support this design philosophy. Past research shows that for practical geometries and proportions of bridge I-girders, there is no significant interaction between bending and shear (White et al. 2001, White et al. 2008, White 2008). Similarly, the strength checks corresponding to the point load action, i.e., web yielding and web crippling, are conducted without combining them with flexure and shear effects. In summary, AASHTO (2014) requires the following verifications, as separated checks:

- Compression flange yielding $\qquad$ $f_{bu} + f_\ell \le \phi_f R_h F_{yc}$
- Compression flange stability $\qquad$ $f_{bu} + f_\ell / 3 \le \phi_f R_h F_{nc}$
- Web bend-buckling $\qquad$ $f_{bu} \le \phi_f F_{crw}$
- Tension flange yielding $\qquad$ $f_{bu} + f_\ell \le \phi_f R_h F_{yt}$
- Web shear strength $\qquad$ $V_u \le \phi_v V_{cr}$
- Web local yielding $\qquad$ $R_u \le \phi_b R_{ny}$
- Web crippling $\qquad$ $R_u \le \phi_b R_{nc}$

This paper presents the studies of a steel I-girder bridge erected with the ILM. Strain/stress measurements in different girder cross-sections are compared to the predictions obtained from

analytical solutions to better understand the behavior of a steel bridge erected with this method; in particular, the stress concentrations that occur due to the combined effects of bending, shear, and patch loading (or M-V-P interaction) near the cantilever support. The results of the field studies also serve to evaluate current models available to calculate the resistance of I-girders subject to this stress interaction.

2. Case Study Description

Los Pajaros Bridge, located in Quito, Ecuador, is a three-span steel I-girder bridge with a total length of 195m. Figure 2 shows the general dimensions of the bridge, a typical cross-section, and the plate sizes of the girders. The bridge is constructed with two independent structures of four and five girders, as shown in Fig. 2(b). All girders are identical and continuous over the supports. The structures were entirely assembled behind Abutment B and moved forward to cross the valley and the Monjas River using the ILM. This methodology was selected over the other option that consisted in assembling the girders in pairs and placing them over the supports with the use of cranes.

a) Elevation view

b) Superstructure cross-section
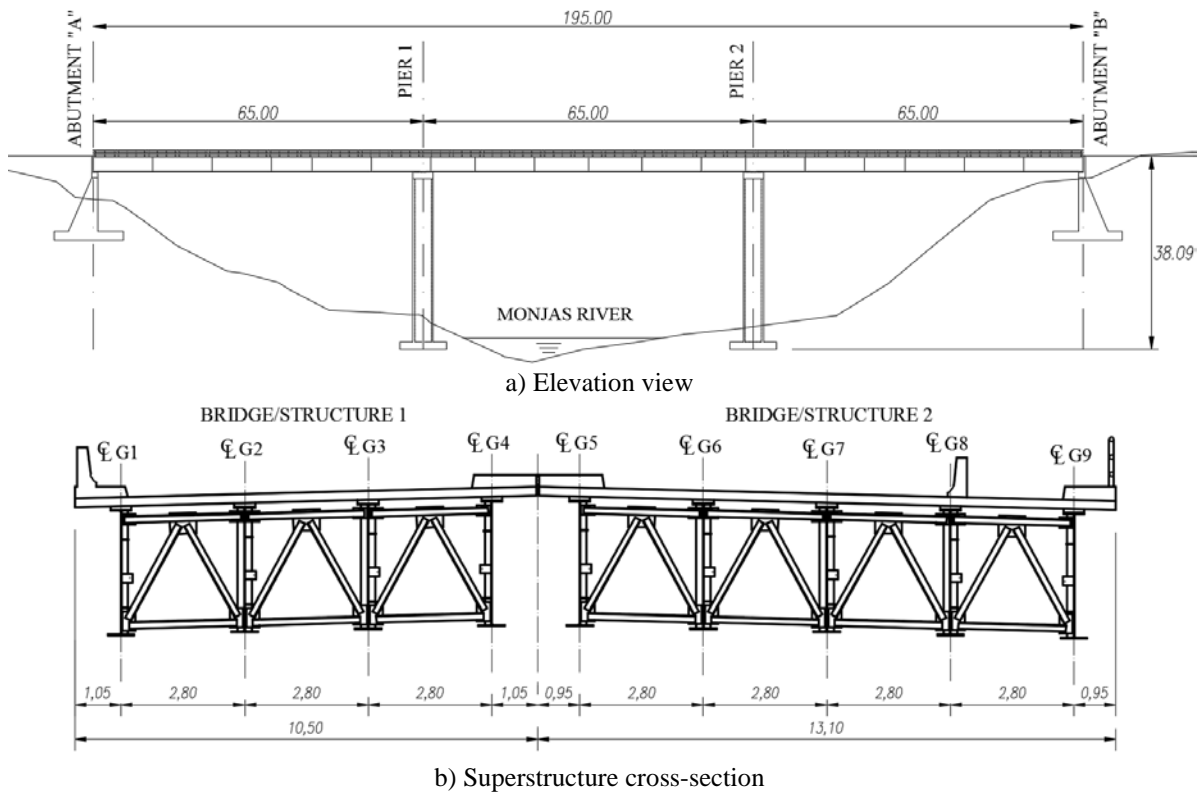
Figure 2: General dimensions and superstructure details of *Los Pajaros* Bridge
(all dimensions in meters unless noted otherwise)

ℂ ABUTMENT "A" ℂ PIER 1 ℂ SYMM. ABT.

SPAN — 65,00 / SPAN 1 — 65,00 / SPAN 2 — SPAN 2

WEB — 43,05 — 11,70 — 20,50 — 11,70 — 21,10
PL 15 x 2800 — PL15 x 2795 — PL 15 x 2775 — PL 15 x 2795 — PL 15 x 2800

TOP FLANGE — 43,05 — 11,70 — 20,50 — 11,70 — 21,10
PL 25 x 470 — PL 30 x 500 — PL 50 x 560 — PL 30 x 500 — PL 25 x 470

0,65

BEARING STIFFENER 2PL 50 x 280

LONGITUDINAL STIFFENER PL 15 x 170

CONNECTION PLATE PL 15 x 150

0,60

STIFFENERS — 9@1,67=15 — 6@2,5=15 — 9@1,67=15 — 9@1,67=15 — 6@2,5=15
4@1,25=5 — 4@1,25=5 — 4@1,25=5
8@0,625=5 — 16@0,625=10

CROSS-FRAMES — 13@5,0=65,0 — 6@5,0=30,0 — 5,0

BOTTOM FLANGE — 43,05 — 11,70 — 20,50 — 11,70 — 21,10
PL 25 x 600 — PL 30 x 600 — PL 50 x 600 — PL 30 x 600 — PL 25 x 600

*PLATE SIZES IN mm

c) Girder elevation
Figure 2 (continued): General dimensions and superstructure details of *Los Pajaros* Bridge
(all dimensions in meters unless noted otherwise)

Some of the benefits of the ILM are that all operations are conducted on firm soil, there is no need to locate any construction items in the sloped terrain, and it is significantly faster than the other method. For these reasons, the ILM was selected for the construction of this structure, and specific design features were implemented in the steel structure geometry to facilitate the launching process. LaViolette et al. (2007) present a thorough discussion of particular aspects that need to be considered for successfully implementing ILM in steel girder bridges. These recommendations were considered in the design of *Los Pajaros* Bridge.

The launching sequence is shown in Fig. 3(a). For the field assembly behind Abutment "B", temporary supports are constructed every 50m approximately, providing five contact points along the length of each girder. These supports have a Teflon pad that facilitates the sliding of the structure while it is being launched. Strand jacks are installed in the abutment to pull the structure, then it slides over pivot bearings mounted at the abutments and the piers. Also, a launching nose is installed at the end of the steel structure to facilitate the operations. As launching progresses, the girders deflect downward in the cantilever. The nose, with its tapered shape, compensates these deflections so that its tip is not under the level of the bearings mounted on the piers and abutments. In addition, the nose reduces the cantilever length in the girders to a maximum of the span length minus the nose length. As a result, the girder stresses and deflections are considerably reduced, as compared to the values obtained if the bridge is launched without a nose. Figure 3(b) shows a photograph of the launching of the first four girders.

5
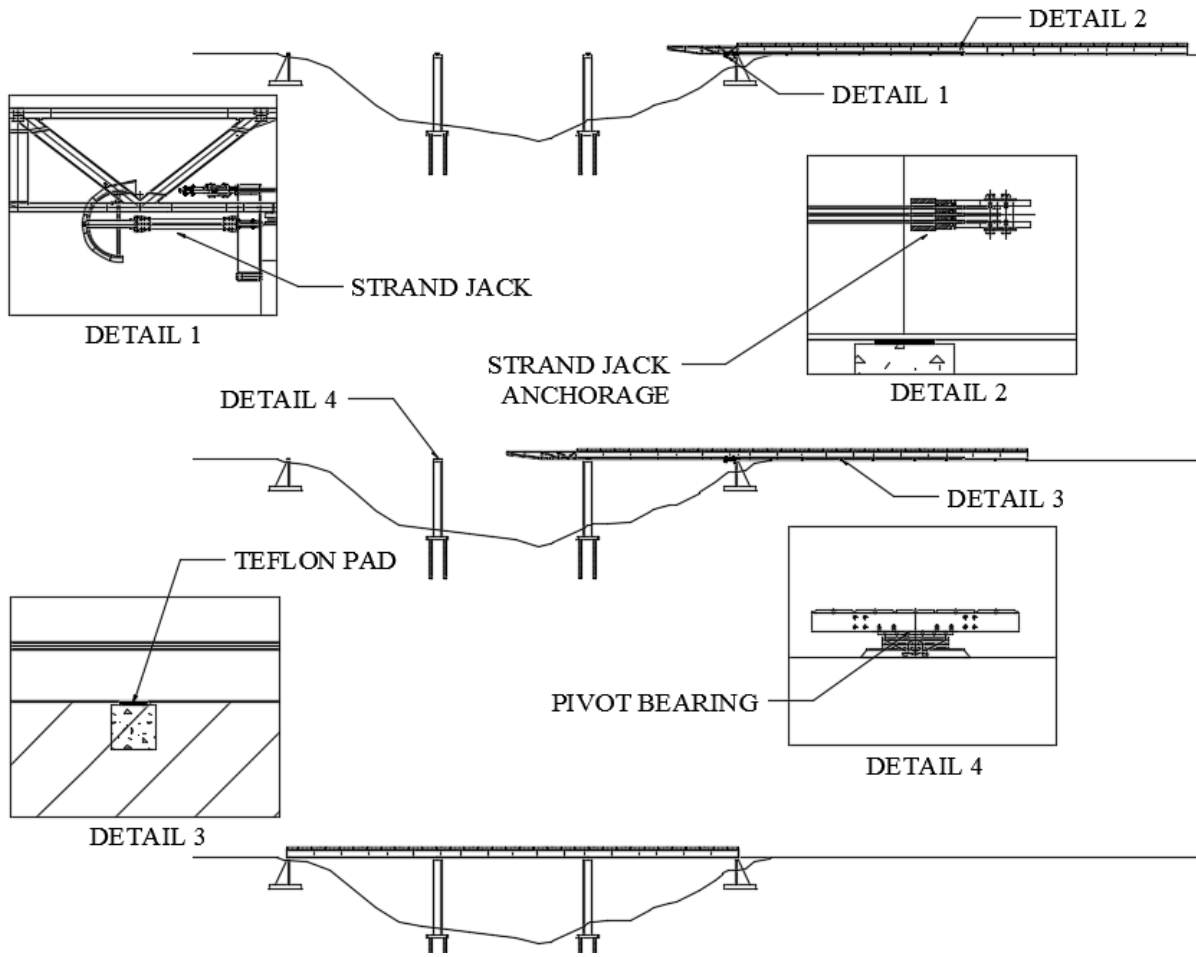
(a) Schematic representation of the launching process

DETAIL 2

DETAIL 1

STRAND JACK

DETAIL 1

STRAND JACK ANCHORAGE

DETAIL 2

DETAIL 4

DETAIL 3

TEFLON PAD

PIVOT BEARING

DETAIL 4

DETAIL 3

(b) Launching of the four-girder structure
Figure 3: ILM of the *Los Pajaros* Bridge

3. Field Instrumentation during Construction

The case study was instrumented with 20 strain gauges known as vibrating wires. The vibrating wires were connected to a data logger with multiple channels that collected the strain measurements during launching. The gauges were placed in three sections along girder G7 at 10m, 25m, and 40m, measured from the girder end, as depicted in Figure 4(a). For identification purposes, these three sections are named as S1, S2, and S3, respectively. Figure 4(b) shows a typical cross-section of the girder and the instrumentation at S2 and S3. Seven vibrating wires were installed at these two sections: two at the top flange, two at the bottom flange, and three at the lower part of the web. The two gauges per flange are useful for separating major-axis bending stresses, f_{bu}, from flange lateral bending stresses, f_ℓ. In general, the f_{bu} stress at the gauges location (i.e., flange inner surface) is equal to the average of the stress measurements. Even though the bridge is straight, there is a minor source of f_ℓ stresses due to the wind pressure that needs to be separated from the f_{bu} stresses to properly capture the responses associated with the launching process only.
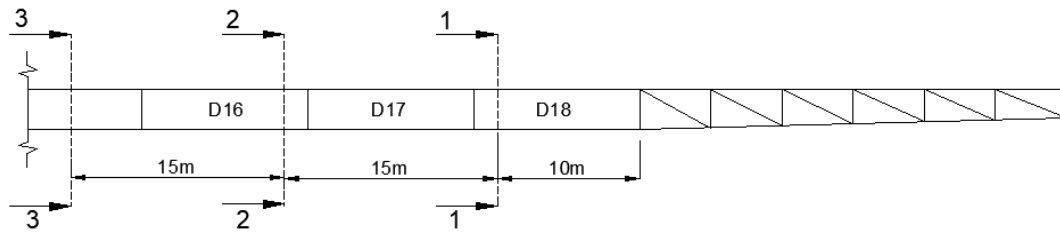
(a) Location of sections S1, S2, and S3
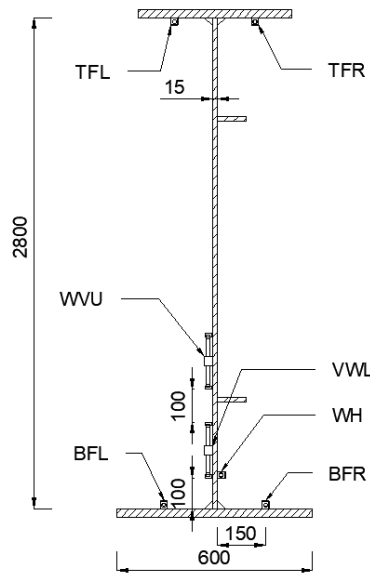
(b) Vibrating wire positions at a typical cross-section
Figure 4: Instrumentation located at three cross-sections along G7

Sections S2 and S3 had three gauges mounted in the web (WVU, VWL and WH), as shown in Fig. 4(b); S1 had only two gauges in the vertical direction (VWL and WVU). These vibrating wires are located as close to the bottom flange as possible to capture the stress concentrations that occur when the sliding surface gets in touch with the girder at the cantilever support. Also, the position

7

of these gauges is convenient to capture the stress contour at the web when the point load is acting on the girder. Figure 5 shows the installation of the instruments in the actual structure.

For measuring the structural responses, the data logger sends a pulse to the gauges. The wire inside of the tube vibrates depending on the level of tensioning, and the data logger records the vibration frequency in B_{units}. As launching proceeds, the wire tension changes, and the natural frequency changes accordingly. To obtain the strain in the element, the B_{units} are multiplied by a calibration factor, F_c, supplied by the manufacturer such that

$$Strain_{\mu\varepsilon} = B_{units} \times F_c \tag{1}$$

Finally, the measurements are transformed to stresses by multiplying the strains by the Young's modulus of steel, i.e., 200GPa, since all deformations during the entire construction process are elastic.
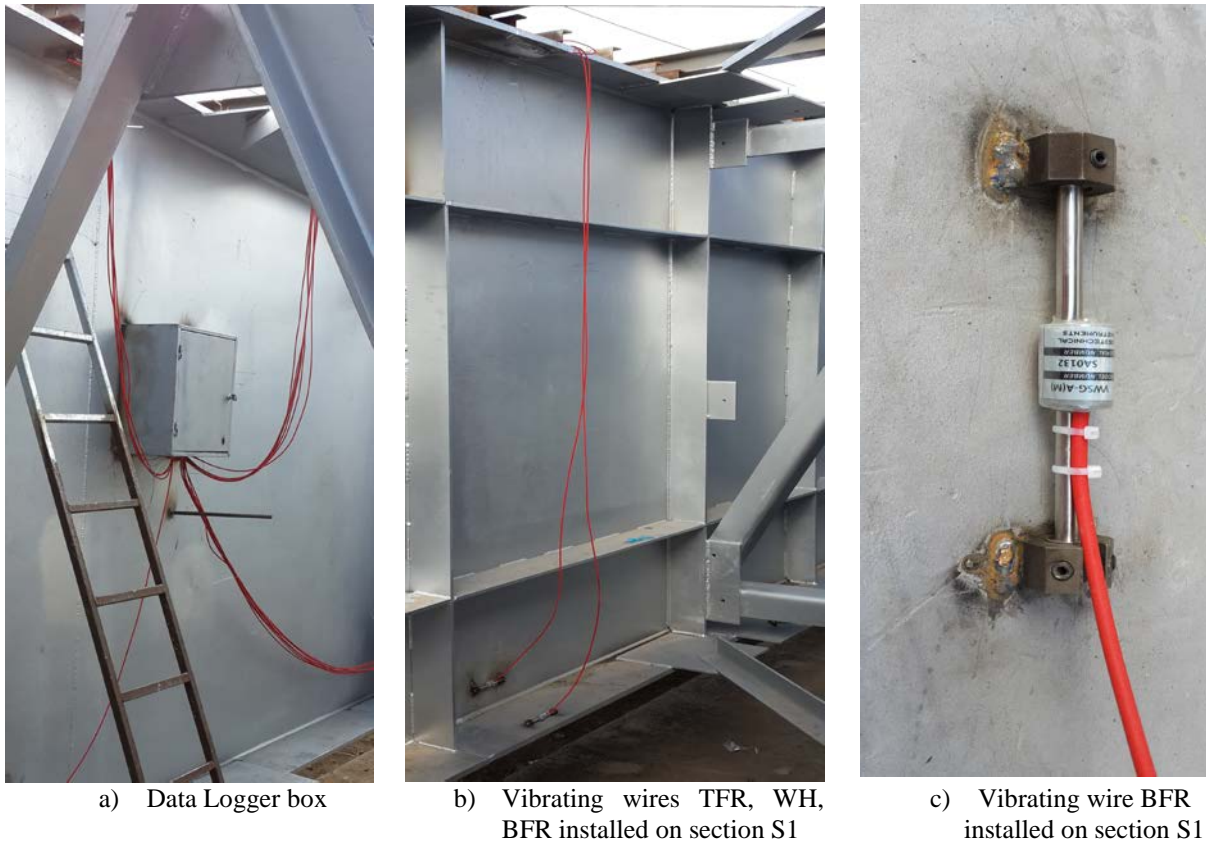
a) Data Logger box   b) Vibrating wires TFR, WH,   c) Vibrating wire BFR
                                 BFR installed on section S1   installed on section S1
Figure 5: Data acquisition system installed on *Los Pajaros* Bridge

In addition to the strain/stress measurements, the vertical deflections at the girder end and the nose were monitored during launching with a total station. As the bridge moves forward, the deflections are tracked and compared to the predictions obtained with the analytical models. Checking this response is necessary to verify the structure's expected behavior as the cantilever length increases.

Section 5 presents the field results obtained with the instrumentation and a comparison with analytical models.

4. Finite Element Model Description

Finite element analyses (FEA) of the case study were conducted to observe the structure's behavior during the launching process. In the numerical analyses, girder webs were modeled with general purpose shell elements. A total of 20 elements are used throughout the depth of the web to properly capture the stress distribution, mainly, at the cantilever support. Girder flanges, transverse and longitudinal stiffeners, and cross-frames are modeled with two-node beam-type elements. The launching nose parts are modeled with truss-type elements to represent the truss behavior that the nose exhibits when bearing on the sliding surfaces located at the abutments and piers. Figure 6 shows the three-dimensional model of the bridge, and a typical stress contour that highlights the stress concentration at the cantilever support. Further details on the FEA characteristics are found in Kim (2010) and Ponton et al. (2016).
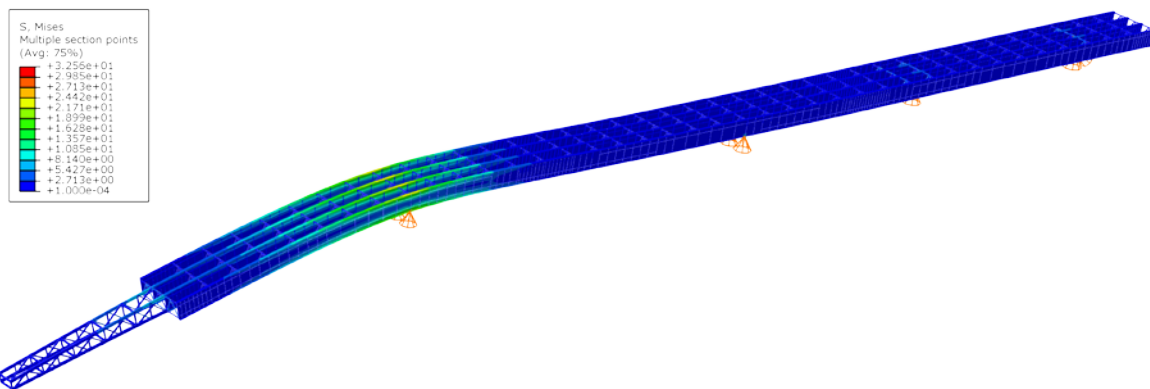
Figure 6: Deformed shaped predicted by the FEA, and von Mises stresses at a cantilever length of 40m. Deflections scaled by a x5 factor.

5. Comparison of Predicted versus Measured Bridge Responses during Launching

Two structural responses were monitored during the launching process: girder vertical deflections at the cantilever end and girder stresses, as discussed in previous sections. Figure 7(a) shows the comparison between the analytical model and the deflection measurements at the free end of girder G7. As shown in the figure, the measured maximum deflection in the first span is 577mm when the cantilever length is 40m. At that point, the 25m-long launching nose lands on the sliding surface at Pier 2, and the deflection recover starts until the girders reach Pier 2. The same behavior is observed as the bridge moves longitudinally, with maximum deflections of 557mm and 540mm in the second and third spans, respectively. The deflections predicted by the FEA are similar to the field measurements, which is an indicator that the bridge was behaving as expected during the launching process.

Figures 7(b) and 7(c) show the stress levels at S3 as a function of the launching length. As in the case of the girder deflections, the solutions obtained with the analytical model are reasonable predictions of the measured values. The plots highlight the significant stress levels that the girders experience during launching. The maximum (tension) stress at the top flange is 196MPa; similarly, at the bottom (compression) flange, the minimum stress is 171MPa. Even though the structure

9

behaved elastically at all stages and no limit state was exceeded (Ponton et al. 2016), the measurements show that bridges erected with the ILM are subject to considerable stresses levels.
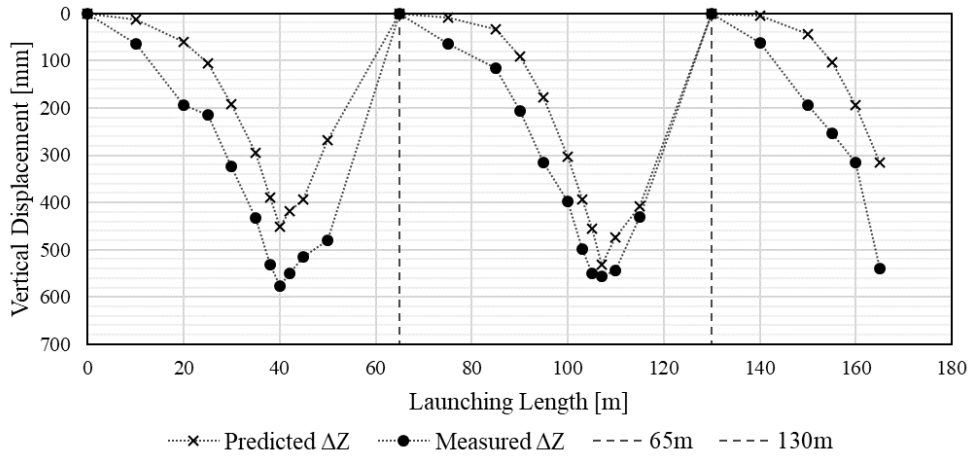
a) Vertical displacement at the end of the girder
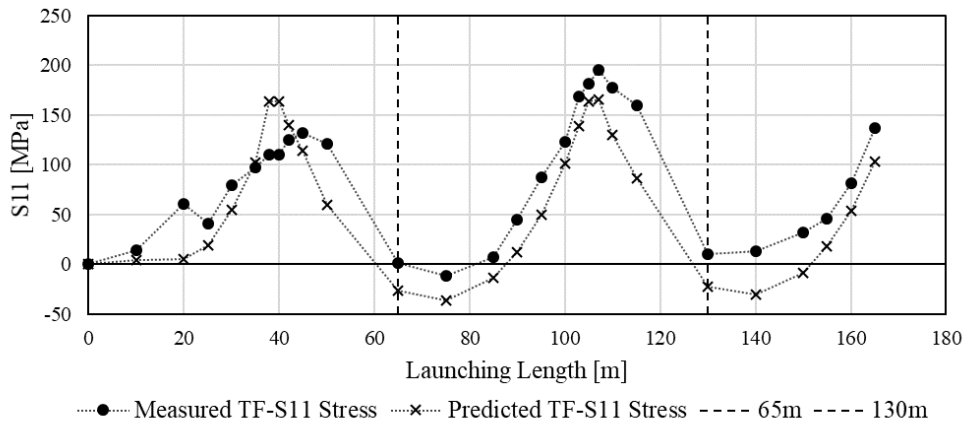
b) Top flange major-axis bending stress – Section S3
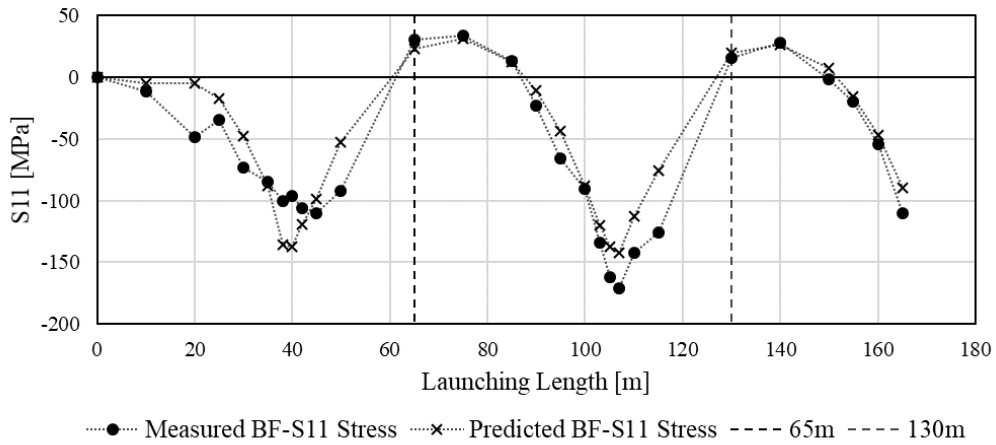
c) Bottom flange major-axis bending stress – Section S3
Figure 7: Predicted versus measured bridge responses during launching
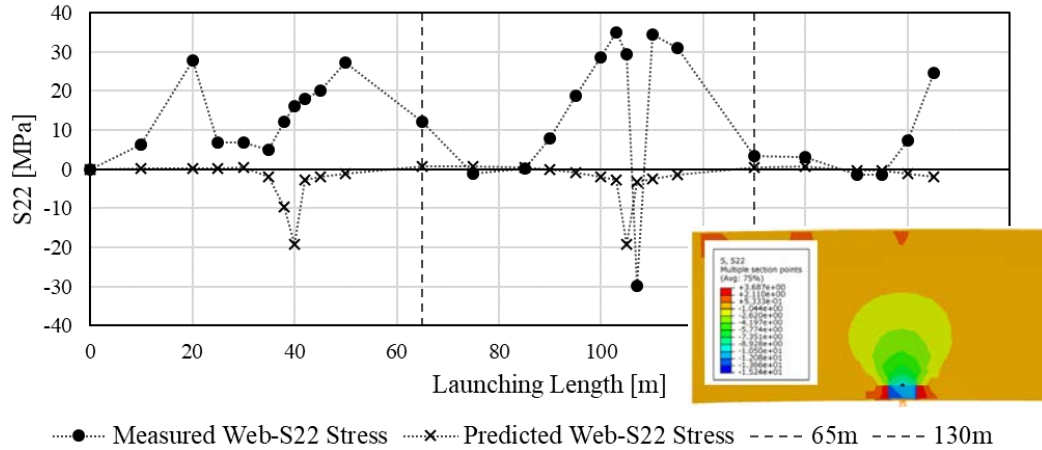
d) Web compression stress – Section S3

Figure 7 (continued): Predicted versus measured bridge responses during launching

Figure 7(d) shows the stress analytical predictions and field measurements at the girder web. In this case, the trend of the FEA results does not follow the same trend of the strain gauge values. The reason is that this response is more complex to measure and has a high sensitivity to the launching length versus the flange stress measurements. As depicted in the stress contour in Fig. 7(d), when the girder is bearing on a support, the web is subject to tension and compression in the same region. Therefore, the web stresses change from tension to compression and vice versa with even a small change of the launching length. The plot, however, shows that in general, the stress range varies between 35MPa in tension and 30MPa in compression.

The field measurements and the FEA predictions show that the I-girders are subject to considerable stress levels during the launching process. The major-axis bending stresses are predicted with accuracy by the analytical models, while the predictions of the web stresses are different to the measured with the instrumentation due to the rapid change that occurs in magnitude and sign as the structure is moved forward. In general, both measured and analytical results show that bridges erected with the ILM experience large demands during this process. Only major-axis bending and patch load effects were measured during launching; however, their magnitudes are substantial and combined with the effect of shear, they may subject the girder panels at the cantilever support to stress levels that could compromise the bridge integrity, as the case shown in Fig. 1. Therefore, for bridges erected with the ILM, it is necessary to study the possible interaction that may exist between bending, shear, and patch loading using three-dimensional FEA, as in the case study, or using the interaction equations discussed in the next section.

6. Application of Available M-V-P Interaction Models to Bridges Erected with the ILM
Studies regarding the interaction between various types of loadings started more than three decades ago, and it is still a topic of current research. Most of the investigations were focused on the interaction between two load effects. P-V, P-M, and V-M interaction models were first developed to evaluate girder resistance under combined types of loadings. More recently, Graciano and Ayestarán (2013) analyzed the M-V-P interaction for transversally stiffened steel girders. This research also considered the adequacy of some of the interaction models available in the literature to properly capture the physical behavior of steel I-girders under a combination of load effects.

11

Table 1 summarizes the interaction models available to compute the effects of combined loading types.

Table 1: Previous investigation of two-dimensional interaction M-P, P-V, M-V

Autor(s)	Mathematical Expression	Interaction Type	Equation Number
Zoetemeijer (1980)	$\left(\dfrac{P}{P_R}\right)^2 + \left(\dfrac{V}{V_R}\right)^2 \leq 1$	P-V	(2)
Shahabian and Roberts (2000)	$\left(\dfrac{P}{P_R}\right) + \left(\dfrac{V}{V_R}\right)^2 \leq 1$	P-V	(3)
Kühlmann and Braun (2007)	$\left(\dfrac{P}{P_R}\right) + \left(\dfrac{V}{V_R}\right)^{1.6} \leq 1$	P-V	(4)
Bergfelt (1971)	$\left(\dfrac{P}{P_R}\right)^8 + \left(\dfrac{M}{M_R}\right)^2 = 1$	P-M	(5)
Elgaaly (1983)	$\left(\dfrac{P}{P_R}\right)^3 + \left(\dfrac{M}{M_R}\right)^3 = 1$	P-M	(6)
Ungermann (1990)	$\left(\dfrac{P}{P_R}\right) + \left(\dfrac{M}{M_R}\right) = 1.4$	P-M	(7)
Lagerqvist (1994)	$\left(\dfrac{P}{P_R}\right) + 0.8\left(\dfrac{M}{M_R}\right) = 1.4$	P-M	(8)
Roberts and Shahabian (2001)	$\left(\dfrac{V}{V_R}\right) + \left(\dfrac{M}{M_R}\right)^4 \leq 1$	V-M	(9)
Braun and Kühlmann (2010)	$\left(\dfrac{P}{P_R}\right) + \left(\dfrac{M}{M_R}\right)^{3.6} + \left(\dfrac{V}{V_R}\right)^{1.6} \leq 1$	M-V-P	(10)

As shown in Table 1, the only model available to capture the interaction between bending, shear and patch loading is the one proposed by Braun and Kühlmann (2010). Graciano and Ayestarán (2013) concluded that this interaction model properly captures the behavior of steel I-girders subject to these three loading effects simultaneously. Similarly, a parametric study based on more than 700 numerical models was performed by Kövesdi et al. (2014). The results of this research again, conclude that the three-dimensional interaction model proposed by Braun and Kühlmann (2010) for longitudinally stiffened and unstiffened steel I-girders is an accurate representation of the girder behavior. Kövesdi et al. (2014) determined that the M-V-P interaction equation is a lower bound solution, as compared to the numerical and experimental results; therefore, Equation (10) is a safe representation of the physical behavior and may be used in practice for the design of steel I-girder bridges.

The results of the M-V-P interaction based on the FEA results of the case study and computed with Equation (10) are presented in Fig. 8. Figure 8(a) shows the three-dimensional plot of the M-V-P

responses for the launching of the *Los Pajaros* Bridge. The Equation (10) calculations are conducted with the stresses predicted at the cantilever support for various values of the launching length. The responses have been normalized with respect to the design strength for bending, shear, and patch loading, ϕR_n, calculated as discussed in Section 1. As depicted in this figure, the unity check based on Equation (10) is fulfilled for all launching stages. Also this figure shows that the loadings and the corresponding interaction becomes larger as the structure moves forward and the cantilever length increases. Figure 8(b) shows a comparison between the structural responses corresponding to the FEA predictions and Equation (10). As shown in this plot, the loading levels during the structure's launching are below the surface computed with this equation that, as mentioned before, represents a lower bound solution. This figure demonstrates that the launching process did not cause stress levels that may compromise the integrity of the bridge.
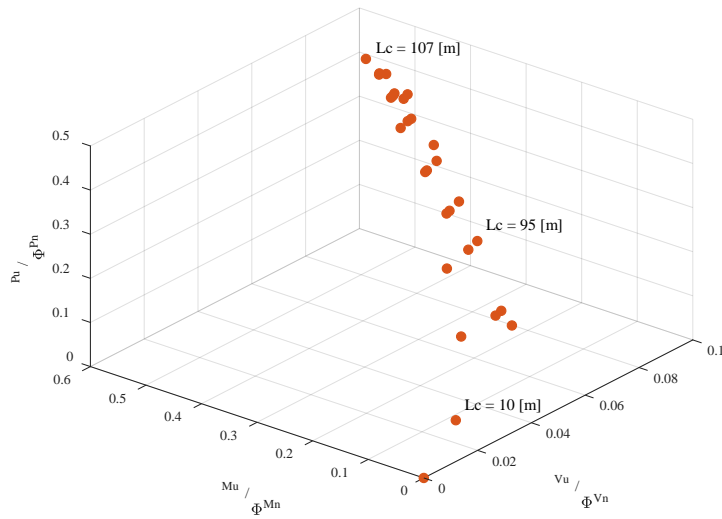
a) 3D plot of the interaction check
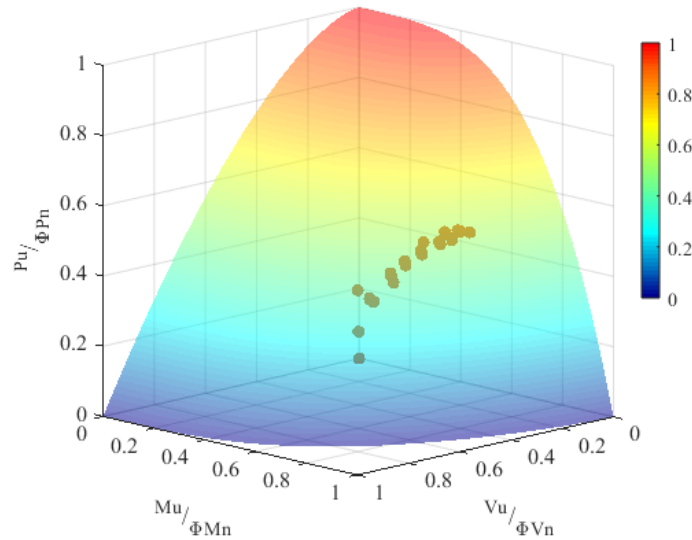
b) Lower bound surface of the Braun and Kühlmann (2010) interaction model

Figure 8: Braun and Kühlmann (2010) interaction check for the launching process of *Los Pajaros* Bridge

7. Conclusions

Bridges erected with the ILM are subject to significant levels of major-axis bending, shear, and patch loading in the regions located at the cantilever support. The combination of these three loading effects may affect the structural performance of the bridge. In extreme cases, the stress concentrations may be large enough to cause the collapse of the structure. This research presents the numerous analytical models that exist to capture the M-V, M-P, V-P, and M-V-P interaction in steel I-girders and their application to bridges erected with the ILM. For this purpose, field measurements of a bridge erected with this method are contrasted with the results obtained with FEA. Both the numerical and physical measurements of the stress responses show that the stress levels are substantial and that the possible M-V-P interaction needs to be studied in detail. The evaluation of the case study with the Braun and Kühlmann (2010) model shows that even though the demands during launching process are high, the bridge was stable and its integrity was not compromised at any stage.

References

AASHTO (2014). AASHTO LRFD Bridge Design Specifications. 7th Edition, American Association of State Highway and Transportation Officials, Washington, DC.

Bergfelt, A. (1971). Studies and tests on slender plate girders without stiffeners – Shear strength and local web crippling. Proceedings, IABSE Colloquium, London, 67-83.

Braun, B., Kühlmann, U. (2010). The interaction behaviour of steel plates under transverse loading, bending moment and shear force. Proceedings of SDSS RIO 2010 stability and ductility of steel structures; p. 731-8 [Rio de Janeiro].

Elgaaly, M. (1983). Web design under compressive edge loads. Engineering Journal AISC, 20 4thQ, 153-171.

Kim, Y. D. (2010). "Behavior and Design of Metal Building Frames Using General Prismatic and Web-Tapered Steel I-Section Members." Doctoral Dissertation, School of Civil and Environmental Engineering, Georgia Institute of Technology, Atlanta, GA, 562pp.

Graciano, C., and Ayestarán, A. (2013). Steel plate girder webs under combined patch loading, bending and shear. Journal of Constructional Steel Research;80:202-212.

Kövesdi, B., Alcaine, J., Dunai, L., Mirambell, E., Braun, B., and Kuhlmann, U. (2014a). Interaction behaviour of steel I-girders Part I: Longitudinally unstiffened girders. Journal of Constructional Steel Research, 103, 327-343.

Kövesdi, B., Alcaine, J., Dunai, L., Mirambell, E., Braun, B., and Kuhlmann, U. (2014b). Interaction behaviour of steel I-girders; part II: Longitudinally stiffened girders. Journal of Constructional Steel Research, 103, 344-353.

Kühlmann, U., and Braun, B. (2007). Combined Shear and patch loading: Numerical studies and development of an interaction equation. Combri-Report-USTUTT-002, Universität Stuttgart, Germany.

Lagerqvist, O. (1994). Patch loading, Resistance of steel girders subjected to concentrated forces. Lulea University of Technology, Div. of Steel and Timber Structures, Publ. S98:3, 1994. Lulea, Sweden.

LaViolette, M., Wipf, T., Lee, Y., Bigelow, J., and Phares, B. (2007). "Bridge Construction Practices Using Incremental Launching." American Association of State Highway and Transportation Officials, Washington, DC.

Ponton, M.E., Robalino, A.F, Sanchez, T.A. (2016). "Stability Considerations for the Construction of I-Girder Bridges using the Incremental Launching Method." Proceedings of the Annual Stability Conference, Structural Stability Research Council, Orlando, FL, 19pp.

Roberts TM, Shahabian F. (2001). Ultimate Resistance of Slender Web Panels to Combined Bending Shear and Patch Loading. J Constructional Steel Res, 57: 779-790.

Shahabian, F., Roberts, T.M. (2000). Combined shear-and-patch loading of plate girders. J Struct Eng, ASCE. 126(3), 316-321.

White, D. W., Zureick, A. H., Phoawanich, N., and Jung, S.-K. (2001). "Development of Unified Equations for Design of Curved and Straight Steel Bridge I-Girders." Final Report to American Iron and Steel Institute Transportation and Infrastructure Committee, Professional Services Industries, Inc., and Federal Highway Administration, School of Civil and Environmental Engineering, Georgia Institute of Technology, Atlanta, GA.

White, D. W., Barker, M. G., Azizinamini, A. (2008). "Shear Strength and Moment-Shear Interaction in Transversely Stiffened Steel I-Girder." Journal of Structural Engineering, American Society of Civil Engineers, Reston, VA, Vol. 134, No. 9, 1437-1449.

White, D. W. (2008). "Unified Flexural Resistance Equations for Stability Design of Steel I-Section Members – Overview." Journal of Structural Engineering, American Society of Civil Engineers, Reston, VA, Vol. 134, No. 9, 1405-1424.

Ungermann, D. (1990). Bemessungsverfahren für vollwand und kastenträger unter besonderer berücksichtigung des stegverhaltens. Stahlbau, RWTH Aachen, Heft 17, ISSN 0722-1037. (In German).

Zoetemeijer, P. (1980). The influence of normal, bending and shear stresses on the ultimate compression force exerted laterally to European rolled sections. Report 6-80-5, Facultiet der Civiele Techniek, Technische Universiteit.